

## Effects of Subcooling on Liquid Wetted Area Fraction of Heater Surface during Nucleate Boiling of Water in a Pool

Youngjae Park <sup>a</sup>, Hyungdae Kim <sup>a\*</sup>

<sup>a</sup> Kyung Hee Univ. Yongin, Gyeonggi 446-701, Republic of Korea

\* Corresponding author: hdkims@khu.ac.kr

### 1. Introduction

Complex two-phase heat transfer phenomena such as nucleate boiling, critical heat flux, quenching and condensation affect the thermal performance of Light Water Reactors (LWRs) under normal operation and during transients/accidents. These phenomena are typically characterized by the presence of a liquid-vapor-solid contact line on the surface from/to which the heat is transferred. For example, in nucleate boiling, a significant fraction of the energy are transferred from a liquid meniscus underneath the boiling bubble through the evaporation and its dynamics [1,2]. Thus, the measurement of liquid-vapor-solid contact line at the edge of the liquid meniscus and dynamics of liquid phase around the bubble are important to explain the boiling heat transfer. Therefore, various measurement techniques for liquid-vapor phase distribution on the heater surface have been developed, such as conductivity and optical probes [3,4], X-ray and  $\gamma$ -ray tomography [5,6], total reflection [7]. Recently, a simple measurement technique to detect the liquid-vapor phase distribution has been developed using infrared thermography, named as DEPIcT or Detection of Phase by Infrared Thermography [8]. In this study, effects of liquid subcooling on the phase distribution during nucleate boiling are investigated.

### 2. Experimental setup

#### 2.1. Brief description on the DEPIcT technique

DEPIcT technique uses difference of the infrared (IR) energy between liquid phase and vapor phase to detect the liquid-vapor-solid contact line. The key feature of this technique is to use an IR transparent heater (e.g. optical grade silicon wafer), and IR-opaque working fluid (e.g. water). The IR camera is located below the heater, while the working fluid lies on upper surface of the heater (Fig. 1(a)). When boiling bubbles exist on the heater surface, the IR camera can distinguish the phase distribution between bubble and liquid, because of the high IR energy from the hot water in contact with the heater and low IR energy from the relatively cold water beyond the bubble. For this reason, the resulting IR image appears dark in dry area and bright in wetted area, as shown in Fig. 1(b). A complete description of DEPIcT technique, including an assessment of its uncertainties is reported in [2,8].

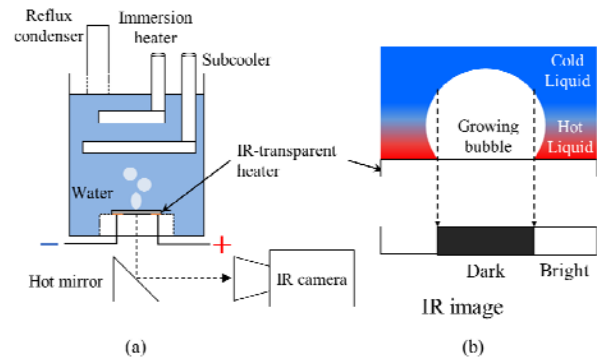


Fig. 1. Experimental apparatus (a) and measurement principle (b) for the DEPIcT technique.

#### 2.2. Boiling experiments

For the subcooled nucleate pool boiling experiments with water at atmospheric pressure, a 30 mm  $\times$  30 mm doped silicon piece as a heater was used with Ti/Au pads for electrical connection to a 600V/30A DC power supply. The boiling chamber has the immersion heater to heat up the working fluid, the reflux condenser to maintain the level and atmospheric pressure, and the subcooler to control subcooling as shown in Fig. 1(a).

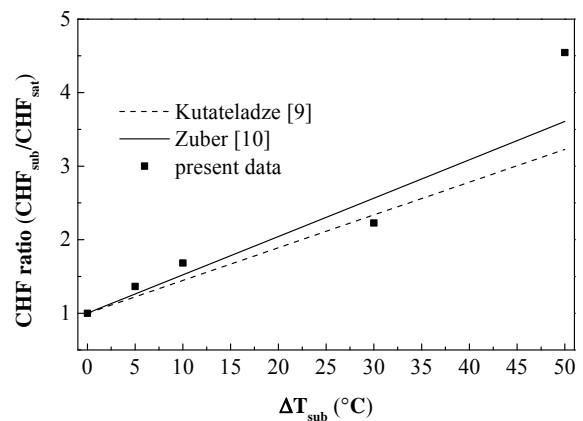


Fig. 2. CHF results of various liquid subcoolings at atmospheric pressure.

### 3. Experimental results

Fig. 2 shows CHF results that normalized to saturated CHF value with degree of water subcooling, and also contains the prediction of CHF values with increasing liquid subcooling using the existing

correlations. The DEPIcT technique could provide insights to interpret effects of liquid subcooling on nucleate boiling and critical heat flux as it permits to determine micro-scale boiling parameters such as the liquid-vapor-solid triple contact line and dry/wetted area. Fig. 3 shows the representative visualization results of the DEPIcT technique for saturated water boiling, which well present the bubble nucleation, merging and vapor retreat (liquid sloshing) phenomena.

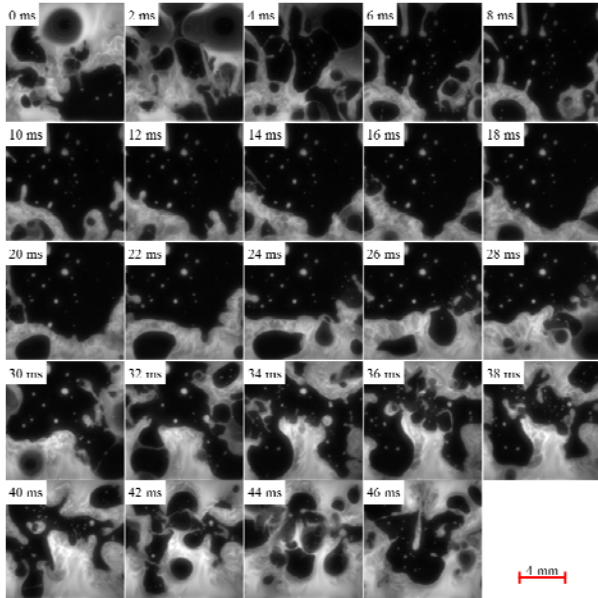


Fig. 3. Snapshot of DEPIcT visualization results for water boiling at  $699.51 \text{ kW/m}^2$ , saturated condition.

Post-processing of the DEPIcT images allows quantification of the wetted/dry area fraction and triple contact line density to interpret boiling phenomena. Fig. 4 and 5 show the time-averaged wetted area fraction and triple contact line density as a function of the normalized heat flux. As the heat flux increases, the wetted area fraction decreases because the number of bubble nucleation increases and individual dry patches underneath boiling bubbles merges together and expands. This tendency is same as those in the previous studies [11,12,13]. In this respect, qualitatively, the triple contact line behavior is expected to be enlargeable and dynamic due to the activation of boiling phenomena (e.g. increasing heat flux), as reported by previous studies [14,15]. Fig. 5 shows the time-averaged triple contact line density as a function of normalized heat flux. The trend of this parameter is monotonically increased with increasing heat flux for all subcoolings, as expected and also reported by reference [14], but not depend on the degree of subcooling. For a given heat flux, there are two contrary effects: (i) the higher subcooling cause the lower value of triple contact line density due to higher wetted area fraction, but (ii) there are also smaller size of individual bubbles (or dry patches), which induce the higher value of triple contact density [2]. In this reason,

the effects of subcooling for triple contact line density are not monotonic. For a given wetted area fraction, however, the latter effect are implies that the high subcooling has a high triple contact line density and small size of individual bubbles, which is shown in Fig. 6 and 7.

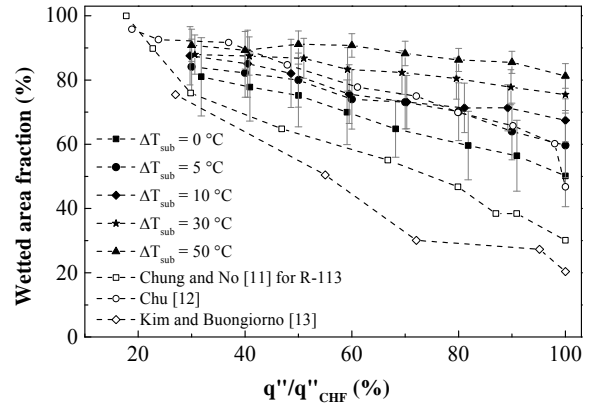


Fig. 4. Time-averaged wetted area fraction as a function of normalized heat flux and liquid subcooling.

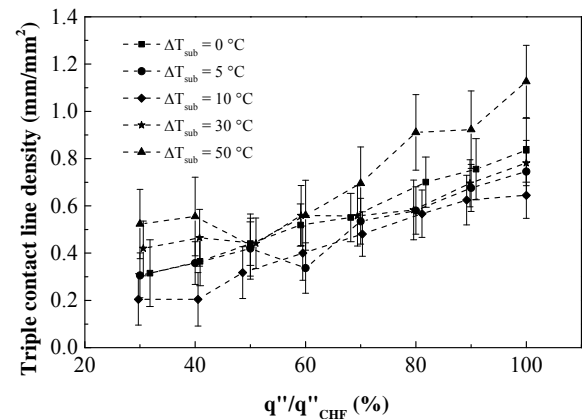


Fig. 5. Time-averaged triple contact line density as a function of normalized heat flux.

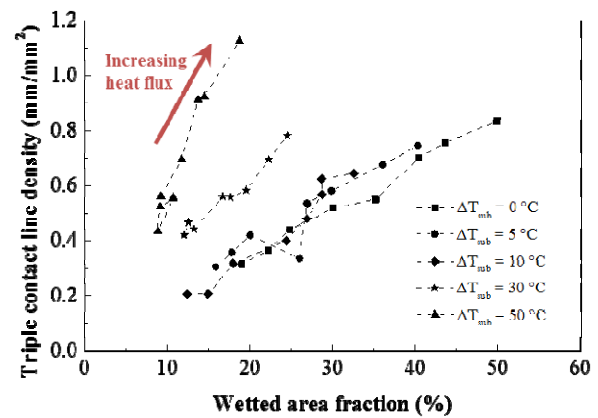


Fig 6. Contact line density vs. dry (or wetted) area fraction as a function of liquid subcooling.

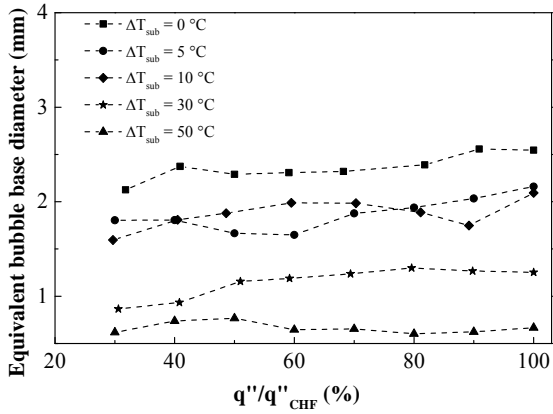


Fig 7. Time and area averaged equivalent bubble base diameter on the heater surface at various subcooling.

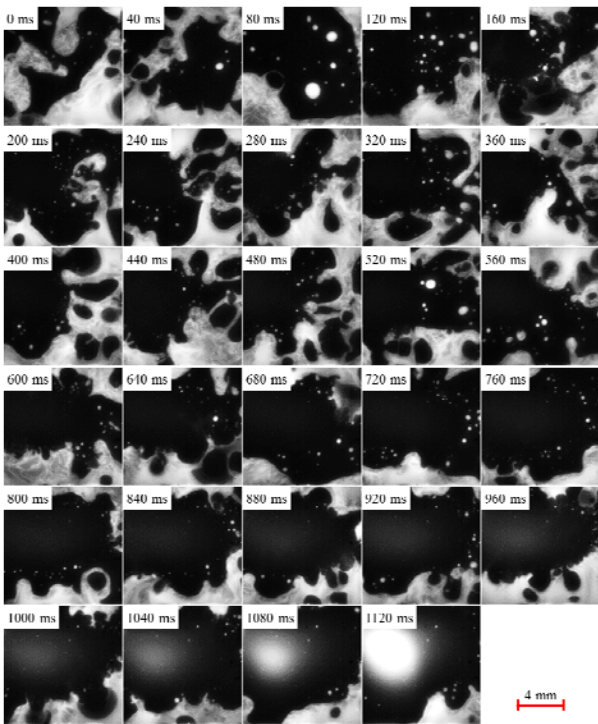


Fig 8. The sequence of CHF occurrence due to the growth of irreversible dry patch during the saturated (0 °C subcooling) nucleate boiling.

#### 4. Discussions

It has been reported by a number of recent studies [2,15,16,17] that critical heat flux phenomenon is triggered by an irreversible growth of a dry patch. And also, our DEPICT technique can observe the CHF phenomenon through the detection of the irreversible dry patch, as shown in Fig. 8.

This phenomenon could be explained by wetted area fraction and triple contact line density. Fig. 9 shows the evolution of dry area fraction and triple contact density at the CHF point. Before the CHF occurs due to irreversible growth of a dry patch, the two parameters have average values with large instantaneous

fluctuations. Then, the both parameters rapidly, in a second, drop down to less than 0.1, which corresponds to film boiling. Table. I shows the transition time from nucleate boiling to film boiling for various liquid subcooling. The transition time is shorter at high liquid subcooling because higher value of CHF (i.e. high thermal energy) with high liquid subcooling.

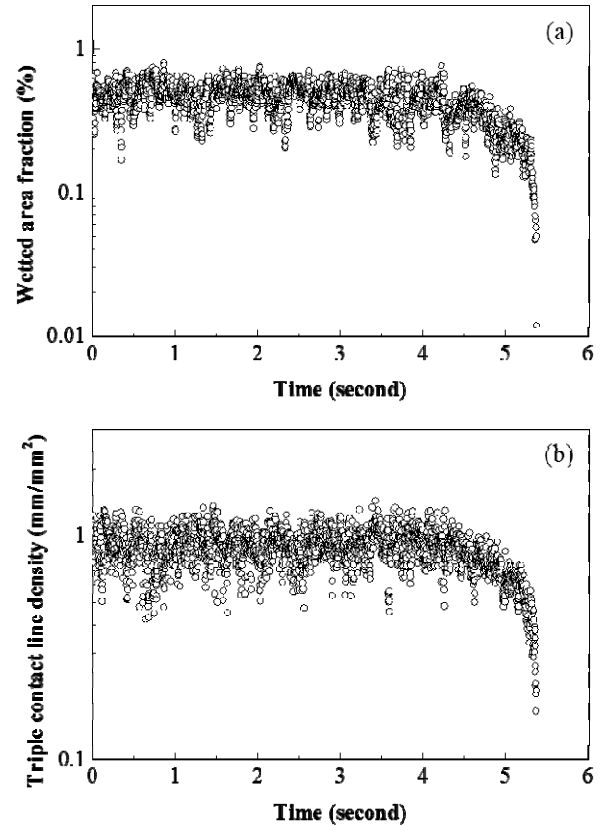


Fig. 9. Instantaneous Fluctuation of wetted area fraction (a) and triple contact line density (b) at CHF condition of

Table I: Transition time of nucleate boiling to film boiling at various liquid subcooling

$\Delta T_{sub}$	0 °C	5 °C	10 °C	30 °C	50 °C
time	~0.7 s	~0.7 s	~0.6 s	~0.4 s	~0.3 s

#### 5. Conclusions

DEPICT technique was applied to measurement of wetted area fraction in pool boiling of water on the smooth surface with various liquid subcooling at atmospheric pressure. The results can be summarized as follows:

- CHF increase with increasing liquid subcooling.
- The wetted area fraction and triple contact line density is measured by DEPICT technique.
- The wetted area fraction decreases with increasing heat flux and decreasing liquid subcooling.

- The triple contact line density increases with increasing heat flux and increasing liquid subcooling.
- The transition time of nucleate boiling to film boiling become shorter at high liquid subcooling.

Future work that would be relevant to nuclear reactor applications includes studying how the wetted area fraction and contact line density depends on water pressure, velocity and surface conditions (e.g. surface wettability or contact angle, roughness, porosity). We are now under investigation to extend DEPICT technique to interpret the effects of micro/nano scale structures on boiling surfaces.

### ACKNOWLEDGEMENT

This research was supported by Basic Science Research Program through the National Research Foundation of Korea (NRF) funded by the Ministry of Science, ICT & Future Planning (No. 2012R1A1A1014779).

### REFERENCES

- [1] T.G. Theofanous, T.N. Dinh, High heat flux boiling and burnout as microphysical phenomena: mounting evidence and opportunities. *Multiphase Science and Technology*. Vol. 18, No. 3, pp. 251-276, 2006.
- [2] H. Kim, Y. Park, J. Buongiorno, Measurement of wetted area fraction in subcooled pool boiling of water using infrared thermography, *Nuclear Engineering and Design*, Vol. 264, pp. 103-110, 2013.
- [3] S. Kim, X.Y. Fu, X. Wang, M. Ishii, Development of the miniaturized four-sensor conductivity probe and the signal processing scheme. *International Journal of Heat and Mass transfer*, Vol. 43 No. 22, pp. 4101-4118, 2000.
- [4] E. Barrau, N. Rivière, Ch. Poupot, A. Cartellier, Single and double optical probes in air-water two-phase flows: real time signal processing and sensor performance. *International Journal of Multiphase Flow*, Vol. 25, No. 2, pp. 229-256, 1999.
- [5] K. Hori, T. Fujimoto, K. Kawamishi, H. Nishikawa, Development of an ultrafast X-ray computed tomography scanner system: application for measurement of instantaneous void distribution of gas-liquid two-phase flow. *Heat Transfer-Asian Research*, Vol. 29, No. 3, pp. 155-165, 2000.
- [6] M. Bieberle, F. Fischer, E. Schleicher, D. Koch, H.J. Menz, H.G. Mayer, U. Hampel, Experimental two-phase flow measurement using ultra fast limited-angle-type electron beam X-ray computed tomography. *Experiments in Fluids*, Vol. 47, No. 3, pp. 369-378, 2009.
- [7] S. Nishio, H. Tanaka, Visualization of boiling structures in high-heat flux pool-boiling. *International Journal of Heat and Mass Transfer*, Vol. 47, pp. 4559-4568, 2004.
- [8] H. Kim, J. Buongiorno, Detection of liquid-vapor-solid triple contact line in two-phase heat transfer phenomena using high-speed infra-red thermometry, *International Journal of Multiphase Flow*, Vol. 37, pp. 166-172, 2011.
- [9] S.S. Kutateladze, Heat transfer during condensation and boiling. Translated from a publication of the State Scientific and Technical Publishers of Literature on Machinery. Moscow-Leningrad, AEC-tr-3770, 1952.
- [10] N. Zuber, M. Tribus, J.W. Westwater, The hydrodynamic crisis in pool boiling of saturated and Subcooled liquid. *Proceeding of International heat transfer meeting*, Vol. 27, pp. 230, 1961.
- [11] H.J. Chung, H.C. No, Simultaneous visualization of dry spots and bubbles for pool boiling of R-113 on a horizontal heater, *International Journal of Heat and Mass Transfer*, Vol. 46, pp. 2239-2251, 2003
- [12] I.C. Chu, Application of visualization techniques to the boiling structures of subcooled boiling flow and critical heat flux, Ph. D. dissertation, KAIST, 2011.
- [13] H. Kim, J. Buongiorno, A novel infrared-based experimental technique to detect phase dynamics on boiling surfaces, *The 14<sup>th</sup> International Topical Meeting on Nuclear Reactor Thermal Hydraulics*, Toronto, Canada, September 25-29, 2011.
- [14] S. Nishio, H. Tanaka, Visualization of boiling structures in high heat-flux pool-boiling. *International Journal of Heat and Mass Transfer*, Vol. 47, pp. 4559-4568, 2004.
- [15] J. Jung, S.J. Kim, J. Kim, Observation of the critical heat flux process during pool boiling of FC-72, *Journal of Heat Transfer*, Vol. 136, pp. 041501, 2014.
- [16] T.G. Theofanous, T.N. Dinh, J.P. Tu, A.T. Dinh, The boiling crisis phenomenon Part II: dryout dynamics and burnout, *Experimental Thermal And Fluid Science*, Vol. 26, pp. 793-810, 2002.
- [17] I.C. Chu, H.C. No, C.H. Song, Visualization of boiling structure and critical heat flux phenomenon for a narrow heating surface in a horizontal pool of saturated water, *International Journal of Heat and Mass Transfer*, Vol. 62, pp. 142-152, 2013.